UNCLASSIFIED

Technical Report #51

(1)

REPORT DOCUMENTATION PAGE

AD-A205 686

DTIC FILE COPY

1a. REPORT SECURITY CLASSIFICATION: NA	1b. RESTRICTIVE MARKINGS: NA
2a. SECURITY CLASSIFICATION AUTHORITY: NA	3. DISTRIBUTION/AVAILABILITY OF REPORT: Distribution Unlimited; Approved for Public Release
2b. DECLASSIFICATION/DOWNGRADING SCHEDULE: NA	
4. PERFORMING ORGANIZATION REPORT NUMBER(S)	5. MONITORING ORGANIZATION REPORT NUMBER(S): NA
6a. NAME OF PERFORMING ORGANIZATION: Indiana University; 6b. OFFICE SYMBOL (If applicable): NA	7a. NAME OF MONITORING ORGANIZATION: ONR
6c. ADDRESS (City, State, and ZIP Code): Department of Chemistry, Bloomington, IN 47405	7b. ADDRESS (City, State, and ZIP Code): 800 N. Quincy Street, Arlington, VA 22217
8a. NAME OF FUNDING/SPONSORING ORGANIZATION; 8b. OFFICE SYMBOL (If applicable)	9. PROCUREMENT INSTRUMENT IDENTIFICATION NUMBER: Contract N00014-86-K-0366
8c. ADDRESS (City, State, and ZIP Code)	10. SOURCE OF FUNDING NUMBERS: PROGRAM ELEMENT NO.; PROJECT NO.; TASK NO. R&T Code 4134006; WORK UNIT ACCESSION NO.

11. TITLE (Include Security Classification): Noise Characteristics of an Inductively Coupled Plasma-Mass Spectrometer

12. PERSONAL AUTHOR(S): N. Furuta, C.A. Monnig, P. Yang, G.M. Hieftje

13a. TYPE OF REPORT	13b. TIME COVERED	14. DATE OF REPORT (Year, Month, Day)	15. PAGE COUNT
Technical	FROM _____ TO _____	February 10, 1989	14

16. SUPPLEMENTARY NOTATION

17. COSATI CODES			18. SUBJECT TERMS (Continue on reverse if necessary and identify by block number)
FIELD	GROUP	SUB-GROUP	Inductively Coupled Plasma; Noise Spectra; Multielement Analysis

19. ABSTRACT (Continue on reverse if necessary and identify by block number)

Noise amplitude spectra for the signal from an inductively coupled plasma-mass spectrometer (ICP-MS) were measured and compared with those obtained with inductively coupled plasma-atomic emission spectrometry (ICP-AES). For the ICP-MS, white noise was dominant in background spectra. An audio-frequency noise peak at 200-350 Hz was observed and behaved much like the one noted earlier in ICP-AES. Unlike in ICP-AES, however, the frequency at which this noise peak occurs is dependent upon the sampling depth in the plasma. Keywords:

20. DISTRIBUTION/AVAILABILITY OF ABSTRACT	21. ABSTRACT SECURITY CLASSIFICATION
☒ UNCLASSIFIED/UNLIMITED ☐ SAME AS RPT ☐ DTIC USERS	Distribution Unlimited
22a. NAME OF RESPONSIBLE INDIVIDUAL: Gary M. Hieftje	22b. TELEPHONE (Include Area Code): (812) 335-2189; 22c. OFFICE SYMBOL

DD FORM 1473, 84 MAR — 83 APR edition may be used until exhausted. All other editions are obsolete.

SECURITY CLASSIFICATION OF THIS PAGE

UNCLASSIFIED

Submitted
Spectrochim Acta
8/89

Noise Characteristics of an Inductively Coupled Plasma - Mass Spectrometer

Naoki Furuta[1], Curtis A. Monnig, Pengyuan Yang and Gary M. Hieftje[2]
Department of Chemistry
Indiana University
Bloomington, IN 47405

---

[1] On leave from: The National Institute for Environmental Studies, 16-2 Onogawa, Tsukuba, Ibaraki 305, Japan

[2] Author to whom correspondence should be addressed.

Abstract

Noise amplitude spectra for the signal from an inductively coupled plasma-mass spectrometer (ICP-MS) were measured and compared with those obtained with inductively coupled plasma-atomic emission spectrometry (ICP-AES). For the ICP-MS, white noise was dominant in background spectra. An audio-frequency noise peak at 200-350 Hz was observed and behaved much like the one noted earlier in ICP-AES. Unlike in ICP-AES, however, the frequency at which this noise peak occurs is dependent upon the sampling depth in the plasma.

1. INTRODUCTION

The reduction of noise is central in any attempt to optimize an analytical measurement. In turn, noise reduction is aided by a knowledge of the origin of the noise and its frequency characteristics (spectra). For inductively coupled plasma atomic emission spectrometry (ICP-AES), noise spectra have been collected and the dominant noise sources identified as either fundamental to the signal itself (ie., shot noise), or as arising from sources involved in the atomization/excitation or gas-flow processes (ie., excess ($^1/_f$), interference, and audio-frequency (AF) noise) [1-6]. While the origin of shot, excess, and interference noise are all relatively well understood, the phenomenon which gives rise to the AF noise remains an area of active controversy. This noise has been postulated to arise from resonances in the ICP torch [1], from the rotation of an asymmetric plasma [2-4], or from vortices induced in the discharge as the support gas passes from the torch [5,6].

Inductively coupled plasma mass-spectrometry (ICP-MS) has received a great deal of attention in recent years as a method for sensitive and selective elemental determinations. Despite the increasing number of reports describing the analytical utility of this instrument, relatively little attention has focused on identifying and understanding the noise sources that affect it. This paper will, for the first time, present noise spectra from an ICP-MS instrument. The similarity and differences between the noise spectra for ICP-MS and ICP-AES instruments will be highlighted. Additionally, the analytical implications of these results will be discussed in the context of proposed applications for this instrumentation.

2. EXPERIMENTAL

2.1. Instrument Description

The ICP-MS used in this study has been described previously [7]. Briefly, a generator (Plasma-Therm Model HFP-2500F, 2.5 kW, 27.12 MHz) and impedance-matching network were used to sustain the ICP. With this instrument, the top turn of the load coil was grounded to minimize the secondary discharge in the first-stage vacuum region of the mass-spectrometer interface. A glass concentric nebulizer and water-cooled Scott double-pass spray chamber were used for sample introduction. Inner and outer gas flows were stabilized with mass-flow controllers (Tylan Corp.). The discharge was sustained in a MAK torch [8] under the conditions listed in Table 1. Mass selection was performed with a quadrupole mass spectrometer (Balzers Model QMG 511) with a nominal mass range of 1 to 511 daltons and unit mass resolution. Detection of the ion current was accomplished with a discrete-dynode secondary electron multiplier (SEM, Balzers Model SEV217). Although this instrument is capable of operating in either an ion-counting or ion-current monitoring detection mode, the work reported here was entirely performed in the ion-current monitoring mode.

Under the operating conditions listed in Table 1, the tip of the initial radiation zone (IRZ) [9] was located at 10 mm above the load coil (ALC), as determined when sodium was aspirated into the discharge. In normal operation, the plasma ions were sampled just above the tip of the IRZ.

The current from the SEM anode was passed directly to a current amplifier (Keithley Model 427), and then through high- and low- pass filters (Krohn-Hite Model 3342, -48 dB/octave roll-off) to eliminate aliasing. When AF noise spectra were acquired (0-500 Hz and 0-1000 Hz frequency range), the high-pass filter was set at 0.1 Hz and the low-pass filter set at 500 Hz and 1000 Hz, respectively. When low frequency spectra (0-10 Hz) were acquired, the high pass filter was bypassed and the low pass filter set to 10 Hz. To permit maximum amplification of the signal noise before digitization, the DC component of the signal was suppressed with the current amplifier.

2.2. Calculation of Noise Amplitude Spectra

A Lab Master data acquisition board (Scientific Solutions) was used to digitize the analog signal for use by an IBM-AT compatible micro-computer (LECO 386). This interface contains a 12-bit A/D converter which was configured to accept input signals between -10 and +10 V. A FORTRAN program controlled data acquisition and calculation of the noise spectrum. Typically, 1024 data points were acquired in each data set, resulting in a noise spectrum containing 512 points. The mean value of each data set was subtracted from each point in the set to suppress any residual DC component of the signal. Noise amplitude spectra were calculated by Fourier transformation of each data set, taking the sum of the square of the real and imaginary components of the transformed data, and signal averaging in the frequency domain. The square root of the averaged spectrum was divided by the current-to-voltage gain of the detection electronics and multiplied by an empirically determined conversion factor to obtain noise spectra directly in units of SEM anode current. Consequently, all amplitude spectra reported here are presented on absolute vertical axes which can be unequivocally compared.

2.3. Reagents

Yttrium and molybdenum standard solutions (1000 $\mu g\ ml^{-1}$) were purchased from Aldrich Chemical Company. These standards were diluted with 0.01 M nitric acid (analytical grade, Mallinckrodt, Inc.) to prepare solutions of the appropriate analyte concentration, and then stored in pre-cleaned polypropylene containers (Nalgene).

2.4. Procedures

The ICP-MS instrument was turned on and allowed to equilibrate for at least two hours prior to the determination of noise spectra. Just before signal acquisition, the ion-optic voltages were adjusted to maximize the ion current of $^{89}Y^{+}$. Under standard operating conditions, an average current

of 32-35 nA was observed for 100 ng ml^{-1} yttrium. Average background currents at a $^{m}/_{z}$ of 89 typically ranged from 5 to 10 pA. As plasma parameters were changed during the course of these experiments, only the ion-optic bias potential [7] was adjusted to reoptimize the ion current.

3. RESULTS AND DISCUSSION

3.1. General Features of Noise Spectra

Several concentrations of $^{89}Y^{+}$ were introduced into the instrument and noise spectra measured. These data are shown in Fig. 1. At high analyte concentrations, an AF noise peak at 266 Hz is observed. As the analyte concentration is lowered, this AF noise peak also decreases. It is clear from Fig. 1 that the background noise of the ICP-MS is random and that white noise is dominant. When the frequency range of the noise spectra were extended to 5 kHz, no significant noise components were observed above 500 Hz. Overall, these traces show the same general features as found previously in ICP-AES noise spectra [1-6].

3.2. Low-Frequency Noise Spectra (0-10 Hz)

Recent work by Hobbs *et al.* [10] demonstrates conclusively that most of the signal excess noise in ICP-AES is associated with the nebulization and vaporization processes and is not related to molecular fragmentation or atomic excitation. It is not unreasonable to assume that the noise in this spectral region would be similar in ICP-AES and ICP-MS instruments.

Figure 2 shows the noise amplitude spectra obtained over a frequency range from 0-10 Hz. A low-frequency noise peak at 1.9 Hz has been traced to pulsations induced by individual rollers on the peristaltic pump used for sample introduction. Harmonics of this noise peak are apparent at 3.8, 5.7, and 7.6 Hz. Also, a small noise band is observed at 0.19 Hz. This frequency corresponds to one complete revolution of the roller wheel on the pump (10 rollers total). This 0.19 Hz signal appears as sidebands on the noise peaks that are associated with individual rollers.

A more fundamental question which must be asked is how the signal is modulated. Figures 2a and b display the noise spectra for $^{89}Y^{+}$ and $^{98}Mo^{+}$, respectively. Both of these species should indicate directly any noise introduced by the peristaltic pump. Figure 2c shows the noise spectrum for $^{80}Ar_2^{+}$. This species would not be modulated directly by the pump, but instead reflect any change in plasma energy conditions. Surprisingly, the noise amplitude for all three spectra remain a relatively constant fraction of the SEM DC current, implying the noise peaks are more the result of a modulation of plasma excitation/ionization conditions at the sampling orifice, than a modulation of analyte introduction into the discharge. The likely cause for this energy modulation is a pulsation in the aqueous aerosol introduction, and hence plasma solvent loading. The plasma sampling conditions used

in this study should be very sensitive to this source of noise since the discharge is being sampled just above the tip of the IRZ [11]. By sampling in a different location in the discharge, it may be possible to minimize this noise. However, an even more direct solution would be to remove the source of the pulsations. When the peristaltic pump is turned off and the sample introduced into the ICP by simple aspiration, the low-frequency noise peaks attributed to the pump disappear completely (Fig. 2d).

3.3. Audio-Frequency Noise Spectra

AF noise, which was observed at 266 Hz under standard operating conditions (see Fig. 1), was monitored as plasma conditions were altered. As shown in Fig. 3, this noise peak shifted to higher frequencies as the RF power and the outer-gas flow rate were raised. However, the peak frequency does not change appreciably if the inner-gas flow rate is varied. These results are nearly identical to those obtained previously with ICP-AES instruments [1-6]. It can therefore be surmised that the origin of the AF noise is common to both types of instruments.

Several researchers have proposed explanations for the origin of the AF noise peak in ICP-AES. Walden *et al.* [1] hypothesized that resonant frequencies in the torch ultimately give rise to this phenomenon. However, the critical dimension of the torch used in this experiment would produce a frequency much higher than the observed AF signal [1]. Clearly, since the AF noise of the ICP is lower than that of "singing" flames, the ICP torch is too short to directly generate this frequency. Belchamber and Horlick [2] observed the AF noise simultaneously with two monochromators at right angles and found that the digitized signals were 90 degrees out of phase with each other. Based on these observations, they proposed that AF noise was caused by an asymmetrical rotation of the plasma. Following up on this work, Davies and Snook [3,4] constructed a laminar-flow torch with the intention of eliminating this "rotation" noise. Although the laminar-flow torch indeed diminished the noise somewhat, an extended outer tube on the torch was necessary to remove it completely.

High-speed photographs of an ICP presented by Winge [5] and Furuta [6] suggest that vertical pulsations in the plasma could account for the AF noise peak. When the outer tube of the torch was extended beyond the region of observation, the pulsations were visibly reduced, in good agreement with the observation of Belchamber and Horlick [2]. Winge *et al.* [5] has attributed the plasma movement to vortex formation in the flowing gases.

Noise amplitude spectra were acquired at different sampling depths in the plasma and are shown in Fig. 4. When the ICP was sampled inside the IRZ, the AF noise peak was not observed (Fig. 4a) or was extremely weak (Fig. 4b). Excess noise clearly dominates the noise spectrum in this lower region of the plasma. One explanation for this observation is that the observed $^1/_f$ noise is associated with sample desolvation and vaporization which occur in the initial radiation zone [11]. The experiments conducted by Hobbs *et al.* [10] do not rule out this possibility. Furthermore, this

hypothesis is consistent with the observation that different nebulizers produce different excess noise spectra [2]; unmatched nebulizers would probably produce different aerosol size distributions.

As the sampling position is moved through the tip of the IRZ (Fig. 4c), an AF noise peak suddenly appears in the noise spectrum. Interestingly, as the sampling position is moved higher in the discharge (Figs. 4d and 4e), the AF noise shifts to lower frequency. This frequency shift is not observed in ICP-AES [4-6] and its basis is not yet clear. However, one possible explanation is that the presence of the sampling cone disturbs the gas flows which ultimately give rise to the vortex.

At a fixed sampling depth of 10 mm ALC, noise spectra were collected at several different radial positions for $^{89}Y^+$ and $^{80}Ar_2^+$. The noise spectra for $^{80}Ar_2^+$ are shown in Fig. 5. From a close scrutiny of this data, it is clear that the 266 Hz noise peak does not shift appreciably in frequency with radial distance. The same behavior was exhibited by $^{89}Y^+$ ions and is also observed in ICP-AES noise spectra [6]. Surprisingly, harmonics of the fundamental 266 Hz AF noise peak were observed when $^{80}Ar_2^+$ was monitored at a radial position 6 mm from the central axis of the discharge (Fig. 5d). This position corresponds with the boundary of the observed discharge. At all other sampling positions, these harmonics were strongly attenuated. This behavior provides strong supporting evidence that turbulence (vortices) are produced in this boundary region.

4. CONCLUSION

From the noise spectra presented here, several observations can be made. The signal variation associated with this ICP-MS instrument is dominated by noise produced by the inductively coupled plasma ion source. Clearly, the background signal of Fig. 1e contains mostly white noise. Relatively low frequency interference noise (0-10 Hz) is primarily the result of pulsations introduced by the peristaltic pump. An AF noise peak (200-350 Hz) similar to that noted in ICP-AES noise spectra was also seen with the ICP-MS instrument. However, two significant differences were noted between the ICP-MS and ICP-AES noise spectra:

1. With ICP-MS, the AF noise peak shifts to lower frequency as the sampling position is moved higher in the plasma.

2. At the boundary region of the argon plasma, strong harmonics of the AF noise are observed.

Because the AF noise peak constitutes a large portion of the total noise under typical operating conditions, it can have a significant effect on the analytical signal. The very nature of the quadrupole mass analyzer encourages rapid mass scans and peak hopping. When the signal of interest is observed on the same time scale as the interfering noise (4 ms for the AF noise reported here), it would be affected significantly by the noise. To overcome this problem, the signal observation time

should be set long enough to average the AF noise, or short enough, ca. 0.5 ms, to minimize the interference.

ACKNOWLEDGEMENTS

Financial support by the National Science Foundation (Grant CHE 87-22639), BP America, and the Office of Naval Research is gratefully acknowledged. One of the authors (N.F.) wishes to thank the Science and Technology Foundation of Shimadzu for the grant of a travel fellowship. Special thanks to George Vickers for his assistance with the operation of the ICP-MS instrument.

References

[1] G. L. Walden, J.N. Bower, S. Nikdel, D.L. Bolton and J.D. Winefordner, *Spectrochim. Acta* **35B**, 535 (1980).

[2] R.M. Belchamber and G. Horlick, *Spectrochim. Acta* **37B**, 17 (1982).

[3] J. Davies and R.D. Snook, *J. Anal. At. Spectrom.* **1**, 195 (1986).

[4] J. Davies and R.D. Snook, *J. Anal. At. Spectrom.* **2**, 27 (1987).

[5] R.K. Winge, D.E. Eckele, E.L. Dekalb and V.A. Fassel, *J. Anal. At. Spectrom.* in press (1987).

[6] N. Furuta, presented at the 1988 Winter Conference on Plasma Spectrometry, San Diego (1988).

[7] D.A. Wilson, G.H. Vickers and G.M. Hieftje, *Spectrochim. Acta* **42**, 29 (1987).

[8] R. Rezaaiyaan, G.M. Hieftje, H. Anderson, H. Kaiser and B. Meddings, *Appl. Spectrosc.* **36**, 627 (1982).

[9] S.R. Koirtyohann, J.S. Jones and D.A. Yates, *Anal. Chem.*, **52**, 1965 (1980).

[10] P. Hobbs, D. E. M. Spillane, R. D. Snook, and A. P. Thorne *J. Anal. At. Spectrom.*, **3**, 543 (1988).

[11] C.A. Monnig and S.R. Koirtyohann, *Anal.Chem.*, **57**, 2533 (1985).

Table 1. Standard Conditions for ICP-MS Instrument

RF power	1.25 kW
MAK ICP torch	
outer-gas flow rate	10.0 L min^{-1}
intermediate-gas flow rate	1.0 L min^{-1}
inner-gas flow rate	1.0 L min^{-1}
Water-cooled spray chamber	
Glass concentric nebulizer (Meinhard type)	
sample uptake rate (using a peristaltic pump)	0.56 mL min^{-1}
Plasma sampling depth (unless otherwise specified)	10 mm ALC

FIGURE CAPTIONS

Fig. 1 Noise amplitude spectra of $^{89}Y^+$ obtained using different analyte concentrations: (a) 500 ng ml^{-1}, anode current 170 nA; (b) 100 ng ml^{-1}, anode current 34 nA; (c) 50 ng ml^{-1}, anode current 17.5 nA; (d) 10 ng ml^{-1}, anode current 3.8 nA; (e) 5 ng ml^{-1}, anode current 1.8 nA. Ions extracted just above the tip of the IRZ under conditions listed in Table 1.

Fig. 2 Noise amplitude spectra over the frequency range 0-10 Hz obtained with the use of a peristaltic pump: (a) $^{89}Y^+$ (100 ng ml^{-1}), anode current 34 nA; (b) $^{98}Mo^+$ (100 ng ml^{-1}), anode current 8 nA; (c) $^{80}Ar_2^+$, anode current 165 nA; (d) $^{89}Y^+$ (100 ng ml^{-1}), anode current 36 nA, obtained without using a peristaltic pump (sample aspirated naturally).

Fig. 3 The audio-frequency noise peak position of $^{89}Y^+$ as a function of (a) RF power; (b) outer-gas flow rate; (c) inner-gas flow rate.

Fig. 4 Noise amplitude spectra of $^{89}Y^+$ obtained at different sampling depths: (a) 7 mm above the load coil (ALC), anode current 5 nA; (b) 8.5 mm ALC, anode current 24 nA; (c) 10 mm ALC, anode current 35 nA; (d) 13 mm ALC, anode current 7.5 nA; (e) 16 mm ALC, anode current 0.6 nA; (f) 19 mm ALC, anode current 0.05 nA. Note different anode current scale on (e) and (f).

Fig. 5 Noise amplitude spectra of $^{80}Ar_2^+$ obtained at different radial positions: (a) on axis, anode current 170 nA; (b) 2 mm off-axis, anode current 18 nA; (c) 4 mm off-axis, anode current 6.2 nA; (d) 6 mm off-axis, anode current 32 nA; (e) 8 mm off-axis, anode current 2.5 nA. Note difference in frequency axis for spectra (d) and (e).

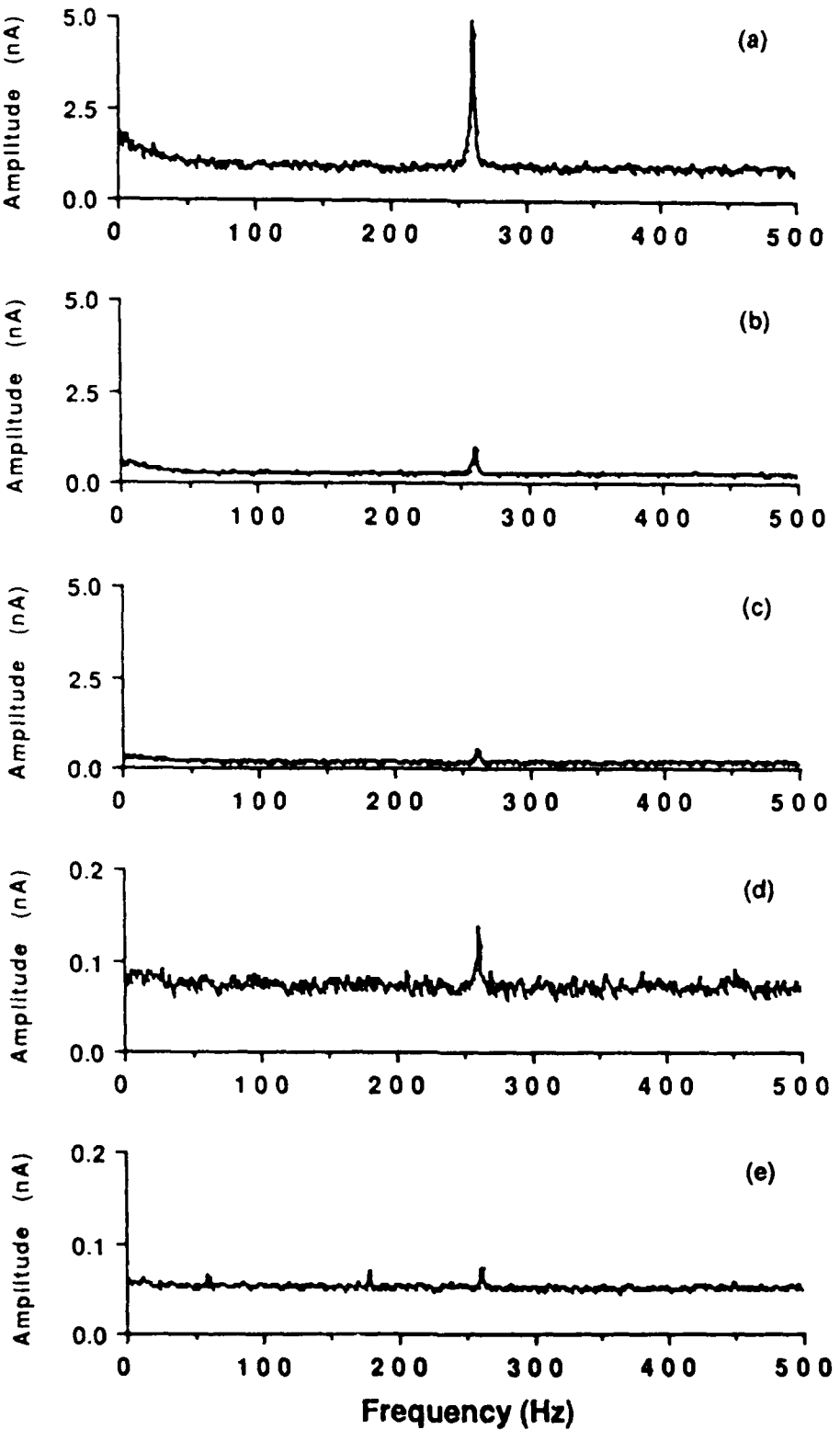
Amplitude (nA)
5.0
2.5
0.0
(a)
0
100
200
300
400
500
Amplitude (nA)
5.0
2.5
0.0
(b)
0
100
200
300
400
500
Amplitude (nA)
5.0
2.5
0.0
(c)
0
100
200
300
400
500
Amplitude (nA)
0.2
0.1
0.0
(d)
0
100
200
300
400
500
Amplitude (nA)
0.2
0.1
0.0
(e)
0
100
200
300
400
500
Frequency (Hz)

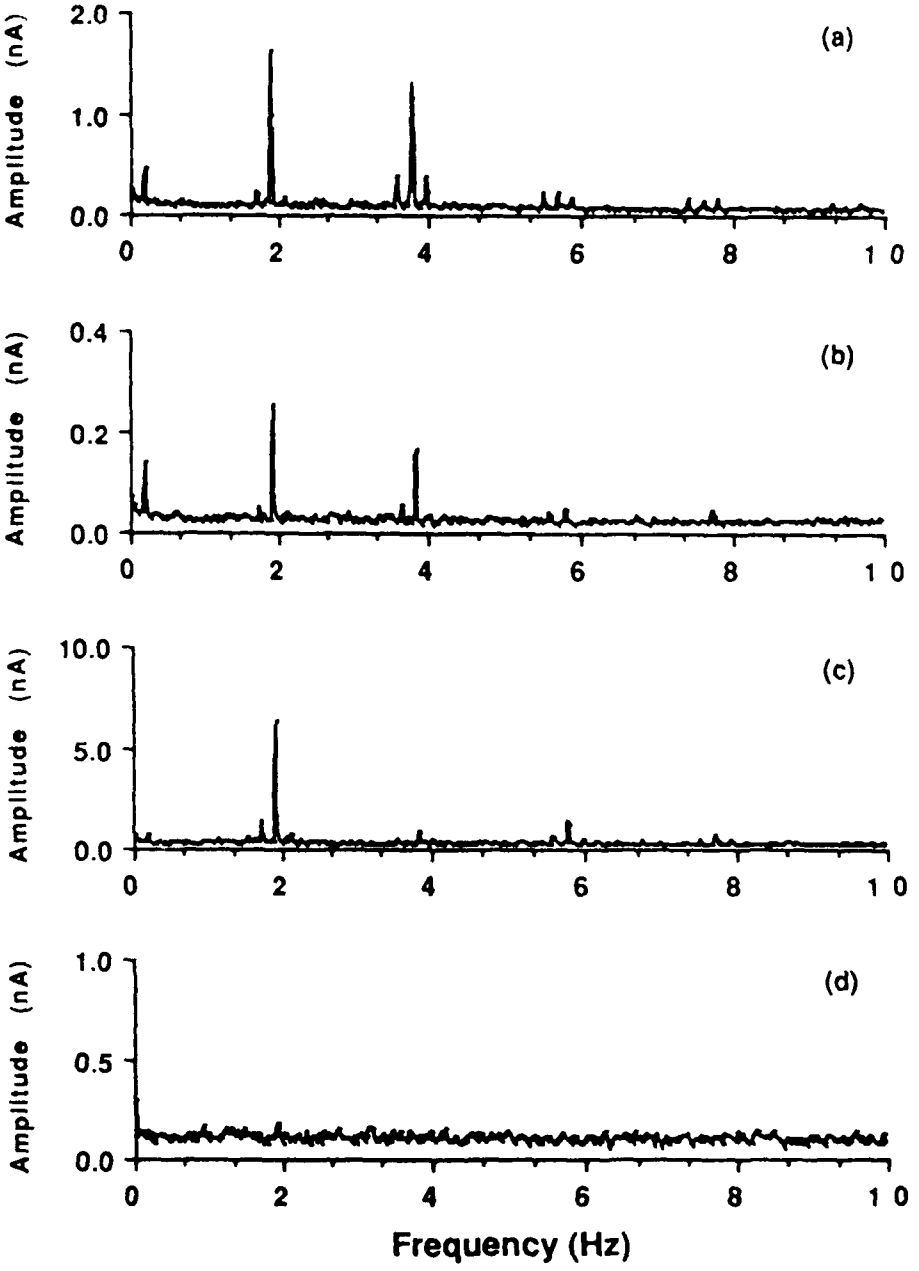
Amplitude (nA)
2.0
1.0
0.0
(a)
0
2
4
6
8
10
Amplitude (nA)
0.4
0.2
0.0
(b)
0
2
4
6
8
10
Amplitude (nA)
10.0
5.0
0.0
(c)
0
2
4
6
8
10
Amplitude (nA)
1.0
0.5
0.0
(d)
0
2
4
6
8
10
Frequency (Hz)

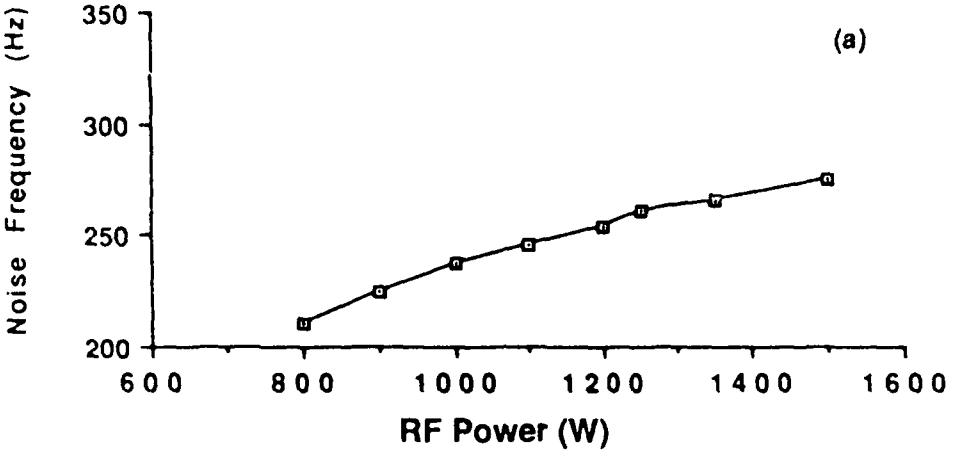
Noise Frequency (Hz)
350
300
250
200
600
800
1000
1200
1400
1600
RF Power (W)
(a)

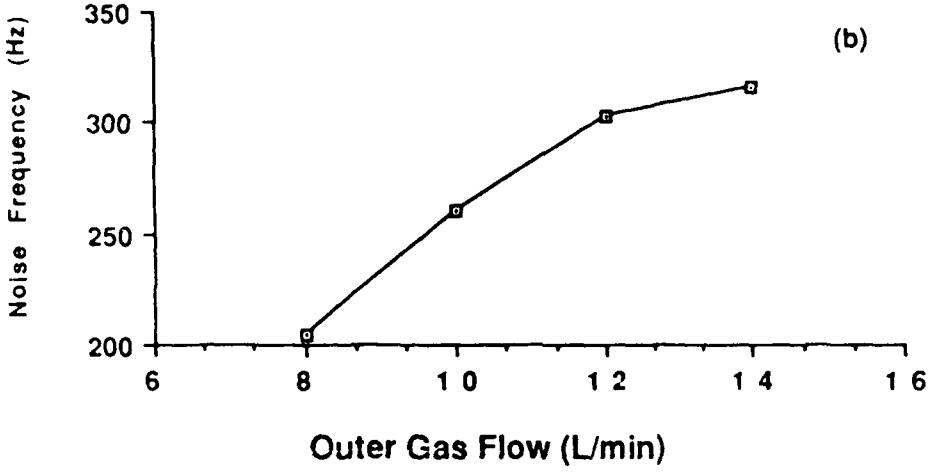
Noise Frequency (Hz)
350
300
250
200
6
8
10
12
14
16
Outer Gas Flow (L/min)
(b)

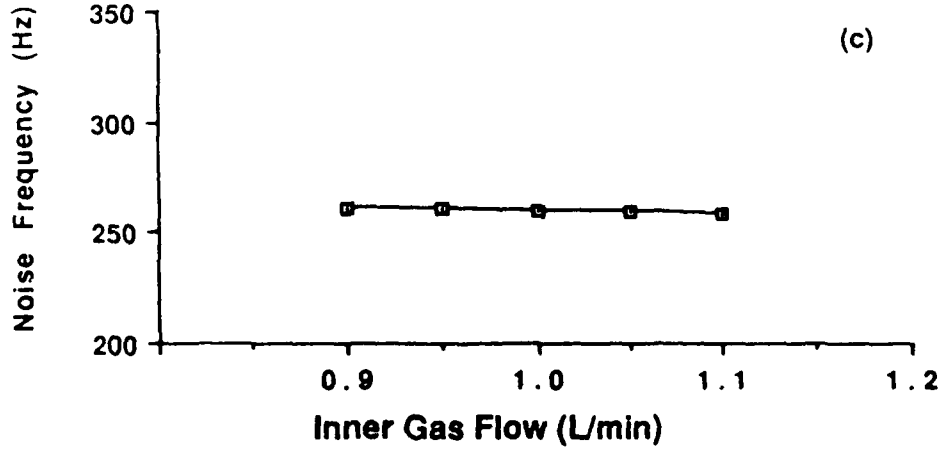
Noise Frequency (Hz)
350
300
250
200
0.9
1.0
1.1
1.2
Inner Gas Flow (L/min)
(c)

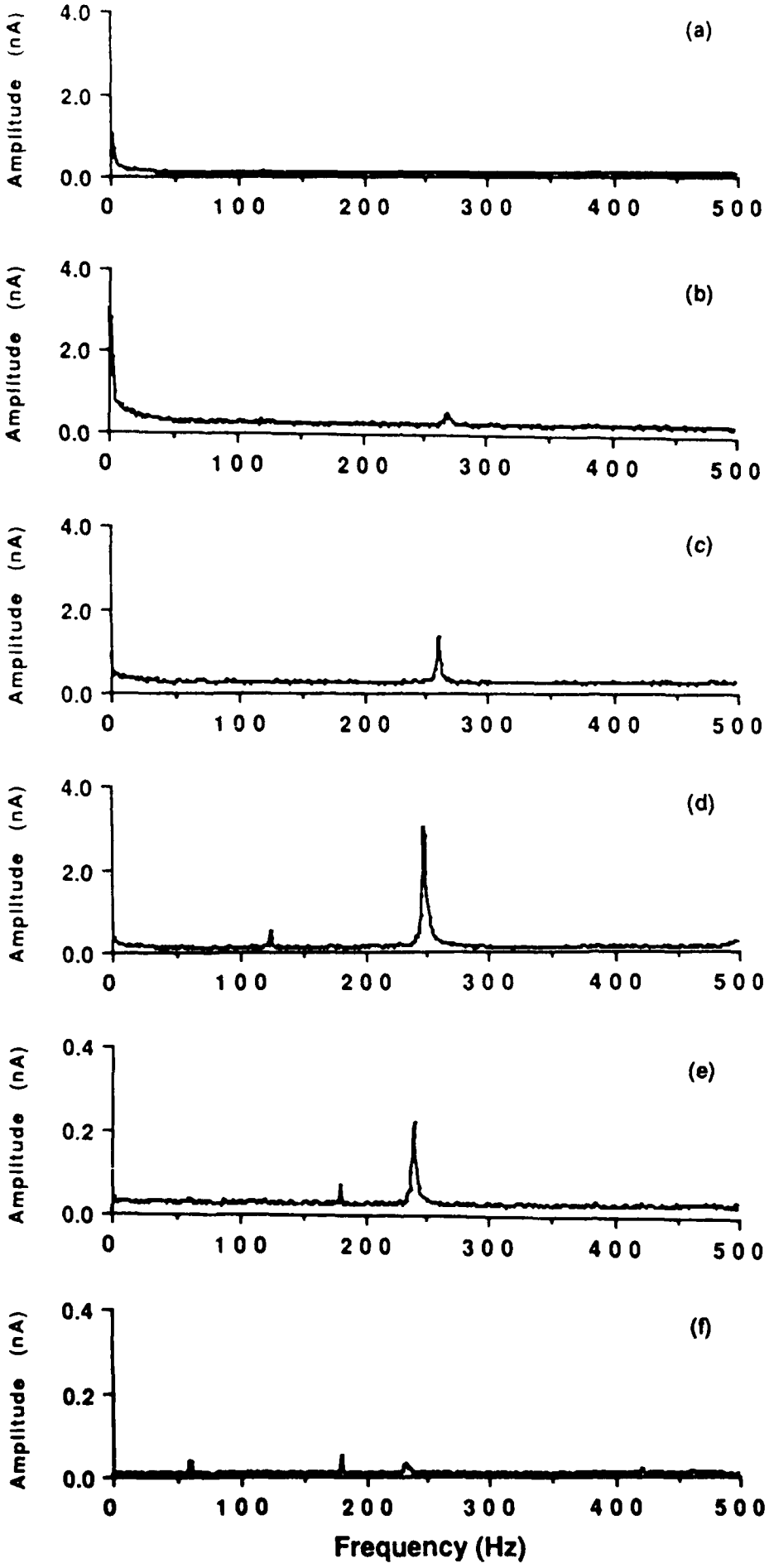
(a)
(b)
(c)
(d)
(e)
(f)
Amplitude (nA)
4.0
2.0
0.0
0.4
0.2
0
100
200
300
400
500
Frequency (Hz)

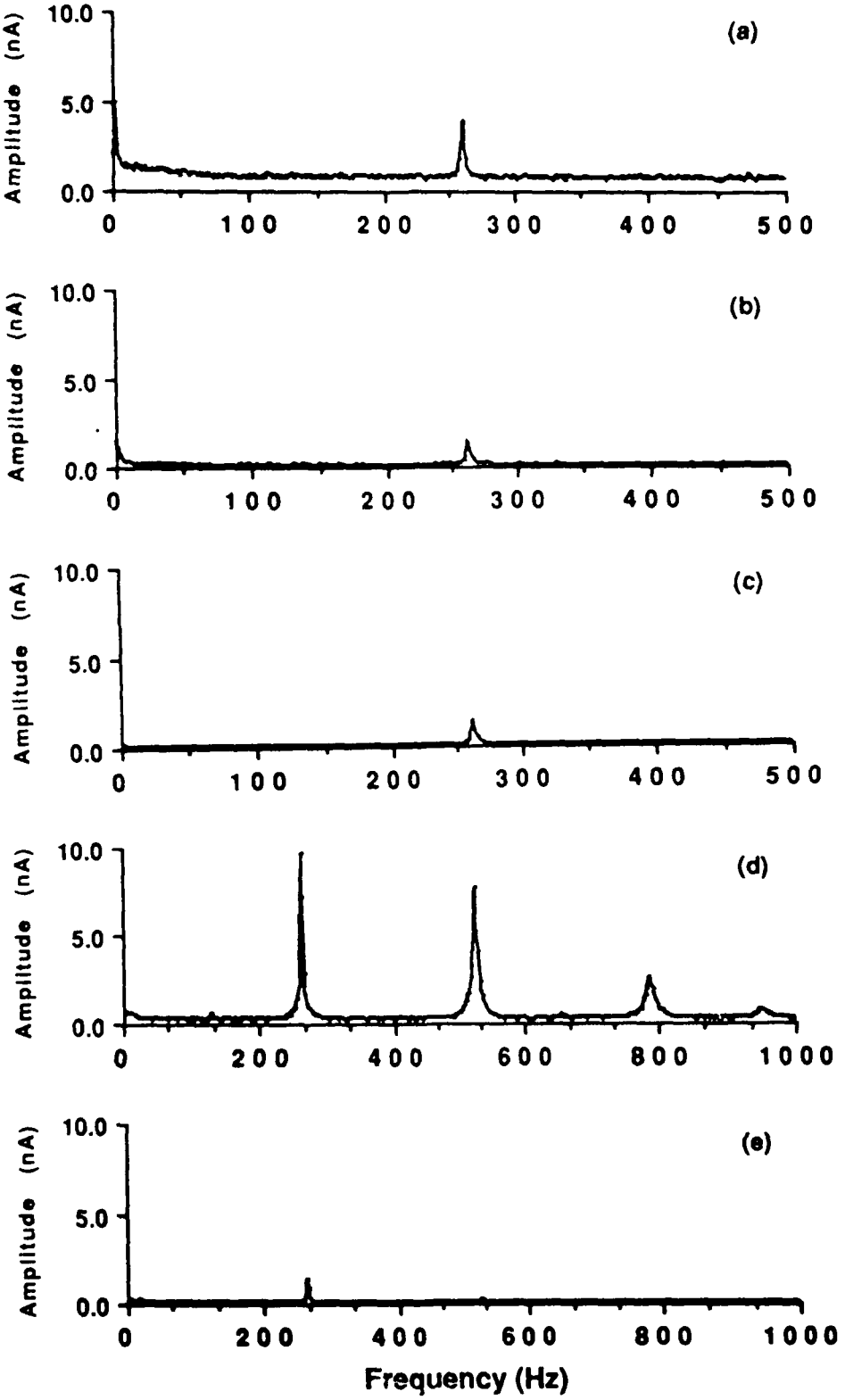
(a)
(b)
(c)
(d)
(e)
Amplitude (nA)
10.0
5.0
0.0
0
100
200
300
400
500
600
800
1000
Frequency (Hz)